Atmos. Chem. Phys. Discuss., 15, 6967–7018, 2015
www.atmos-chem-phys-discuss.net/15/6967/2015/
doi:10.5194/acpd-15-6967-2015

Atmospheric Chemistry and Physics Discussions

Trapping, chemistry and export of trace gases in the South Asian summer monsoon observed during CARIBIC flights in 2008

A. Rauthe-Schöch[1], A. K. Baker[1], T. J. Schuck[1], C. A. M. Brenninkmeijer[1], A. Zahn[2], M. Hermann[3], G. Stratmann[4], H. Ziereis[4], P. F. J. van Velthoven[5], and J. Lelieveld[1]

[1]Max Planck Institute for Chemistry (Otto Hahn Institute), Department of Atmospheric Chemistry, Mainz, Germany
[2]Karlsruhe Institute of Technology (KIT), Institute for Meteorology and Climate Research, Karlsruhe, Germany
[3]Leibniz Institute for Tropospheric Research (TROPOS), Leipzig, Germany
[4]German Aerospace Center (DLR), Institute for Atmospheric Physics, Oberpfaffenhofen, Germany
[5]Royal Netherlands Meteorological Institute (KNMI), De Bilt, the Netherlands

Received: 6 February 2015 – Accepted: 17 February 2015 – Published: 10 March 2015

Correspondence to: A. Rauthe-Schöch (armin.rauthe-schoech@mpic.de)

Published by Copernicus Publications on behalf of the European Geosciences Union.

Abstract

The CARIBIC (Civil Aircraft for the Regular Investigation of the Atmosphere Based on an Instrument Container) passenger aircraft observatory performed in situ measurements at 10–12 km altitude in the South Asian summer monsoon anticyclone between June and September 2008. These measurements enable us to investigate this atmospheric region, which so far has mostly been observed from satellites, using the broad suite of trace gases and aerosols measured by CARIBIC. Elevated levels of a range of atmospheric pollutants were recorded e.g. carbon monoxide, total reactive nitrogen oxides, aerosol particles and several volatile organic compounds. The measurements provide detailed information about the chemical composition of air in different parts of the monsoon anticyclone, particularly of ozone precursors. While covering a range of 3500 km inside the monsoon anticyclone, CARIBIC observations show remarkable consistency, i.e. with regular latitudinal patterns of trace gases during the entire monsoon period. Trajectory calculations indicate that these air masses originated mainly from South Asia and Mainland Southeast Asia.

Using the CARIBIC trace gas and aerosol measurements in combination with the Lagrangian particle dispersion model FLEXPART we investigated the characteristics of monsoon outflow and the chemical evolution of air masses during transport. Estimated photochemical ages of the air were found to agree well with transport times from a source region east of 95° E. The photochemical ages of the air in the southern part of the monsoon anticyclone were consistently younger (less than 7 days) and the air masses mostly in an ozone forming chemical regime. In its northern part the air masses were older (up to 13 days) and had unclear ozone formation or destruction potential. Based on analysis of forward trajectories several receptor regions were identified. In addition to predominantly westward transport, we found evidence for efficient transport (within 10 days) to the Pacific and North America, particularly during June and September, and also of cross-tropopause exchange, which was strongest during June and July. Westward transport to Africa and further to the Mediterranean was the main pathway during July.

1 Introduction

During boreal summer the South Asian monsoon dominates atmospheric circulation over Asia, and has a strong influence on atmospheric transport and chemistry of most of the northern hemisphere (Randel and Jensen, 2013). The monsoon is characterised by a persistent large-scale anticyclonic structure in the upper troposphere, centred over Pakistan and Northern India, framed by the subtropical eastward jet in the north and the westward equatorial jet in the south. This upper troposphere anticyclone (UTAC) is not static but oscillates in strength, shape and position (Garny and Randel, 2013). At the same time it features a remarkably distinct composition signature throughout the monsoon season. Observations from satellites have shown an enhancement of mixing ratios of a number of trace gases in the UTAC, most prominently methane (CH_4) (Xiong et al., 2009) and carbon monoxide (CO) (Kar et al., 2004). Since the monsoon is accompanied by strong convection, upper tropospheric trace gas mixing ratios are directly linked to surface emissions in this densely populated region. In addition, polluted air masses can be trapped and accumulate inside the UTAC, where they can be chemically isolated for several days (Randel and Park, 2006; Park et al., 2008). The UTAC can also play a governing role in the dispersion of volcanic plumes, e.g. after the June 2011 eruption of the Nabro volcano in Eritrea (Fairlie et al., 2014). Outflow occurs predominantly westward towards Northern Africa and the Middle East, where a summertime ozone (O_3) maximum due to ozone formation in monsoon outflow has been reported (Li et al., 2001; Liu et al., 2009), and to the Mediterranean region (Lelieveld et al., 2002; Scheeren et al., 2003). Not only does the South Asian summer monsoon influence the composition of the upper troposphere, it also affects cross-tropopause transport into the lowermost stratosphere (Traub and Lelieveld, 2003; Lelieveld et al.,

2007; Randel et al., 2010; Chen et al., 2012). An extensive review on southern Asian pollution outflow in all seasons is given by Lawrence and Lelieveld (2010).

While most observations in the South Asian summer monsoon UTAC are from satellites, CARIBIC (Civil Aircraft for the Regular Investigation of the Atmosphere Based on an Instrument Container, www.caribic-atmospheric.com, Brenninkmeijer et al., 2007) phase 2 provides the first in situ observations over the Indian subcontinent, performed during the 2008 monsoon season. During the summer monsoon period from June through September, 14 flights between Frankfurt, Germany and Chennai, India, were conducted, crossing the western part of the UTAC at altitudes between 10 and 12 km. The CARIBIC observatory thus provided the comprehensive measurements within the UTAC called for by experts on atmospheric chemistry and the Asian monsoon (Crawford and Pan, 2013). The CARIBIC in situ observations in the upper troposphere aim to contribute to the understanding of the monsoon and its impacts on atmospheric composition (Pan et al., 2014) through this and previous studies (Schuck et al., 2010; Baker et al., 2011).

Elevated mixing ratios of a range of trace gases were measured within the UTAC, for example CO, CH_4, nitrous oxide (N_2O), sulfur hexafluoride (SF_6) (Schuck et al., 2010), several non-methane hydrocarbons (NMHCs, Baker et al., 2011) as well as methyl chloride (CH_3Cl, Umezawa et al., 2014). Furthermore, as earlier measurements from CARIBIC phase 1 have shown, aerosol particle number concentrations are enhanced in the UTAC (Hermann et al., 2003). Trajectory calculations indicated that the air masses originated mainly from South Asia and Mainland Southeast Asia and had been transported up to cruise altitude by deep convection associated with the summer monsoon. High mixing ratios of water vapour at southern latitudes confirmed that recent convection had occurred. An analysis of tracer correlations, namely CO, CH_4 and ethane (C_2H_6), revealed that, in addition to enhanced vertical transport of polluted boundary layer air, emissions of methane from biogenic sources, such as wetlands, open landfills, and rice paddies, increase during the summer months (Baker et al., 2012), resulting in disproportionately high mixing ratios. Carbon dioxide (CO_2) mixing

ratios were found to be lower inside the UTAC. A model study using CARIBIC data found that in 2008 the region was a net sink of CO_2 because of strong uptake by the terrestrial biosphere (Patra et al., 2011). Additionally, $\delta^{18}O(CO_2)$ values indicate oxygen exchange with soil and leaf water (Assonov et al., 2010).

In September 2007, the CARIBIC aircraft also encountered air masses with the typical monsoon signature of elevated mixing ratios of CH_4, N_2O, SF_6 and some NMHCs, accompanied by relatively low CO_2 mixing ratios. In this case it was not over the South Asian monsoon region, but over eastern Canada in the vicinity of Toronto. Air mass trajectories pointed to export from the monsoon region (see Sect. S1 for details), although transport of Asian pollution over the Pacific towards North America occurs predominantly in the northern hemispheric winter and spring (Liu et al., 2003) whereas in summer westward outflow is prevalent. While no comparable case was observed during CARIBIC flights to North America in subsequent years, plumes of photochemically processed air originating from Asia have been probed over different parts of North America during INTEX-NA (The Intercontinental Chemical Transport Experiment – North America) flights in July and August 2004 (Liang et al., 2007).

CARIBIC measurements yield a detailed description of the chemical composition of air in different parts of the UTAC, including mixing ratios of ozone precursors like the sum of reactive nitrogen oxides (NO_y), CO and NMHCs. Using this information and the Lagrangian particle dispersion model FLEXPART (Stohl et al., 2005) we investigate the characteristics of monsoon outflow and the chemical evolution of air masses during transport. Based on analysis of air mass forward trajectories several receptor regions are identified and their relative role is tentatively quantified.

2 Methods

The CARIBIC observatory phase 2 started routine operation in 2005. It is operates on a monthly basis aboard a Lufthansa Airbus A340-600 to make observations during a series of two to six long distance flights. The aircraft is fitted with a permanently

mounted inlet system which is connected via (partially heated) stainless steel tubing to the CARIBIC container when installed. Some of the tubings are lined with thin walled PFA tubes to avoid wall effects (Brenninkmeijer et al., 2007). The 1.6 ton container houses instruments for in situ measurements as well as glass flasks for the collection of whole air samples. Flights start from Frankfurt, Germany, to various destinations around the globe. After the final return flight, the container is unloaded, the measurement data are retrieved and the air samples are analysed for a suite of different trace gases in several laboratories (Brenninkmeijer et al., 2007; Schuck et al., 2009; Baker et al., 2010; O'Sullivan, 2007).

From April to December 2008, the CARIBIC container measured during 32 flights between Frankfurt, Germany and Chennai, India. For this study, we consider only the 14 flights conducted between June and September 2008 (see list of flights in Table 1). These months represent the core of the monsoon period over India in this year as previously discussed by Schuck et al. (2010) and Baker et al. (2011). More information about the non-monsoon months can be found in these two previous studies and will not be discussed here. All 14 flights crossed the western part of the monsoon UTAC over the western coast of India before reaching Chennai at the east coast. The UTAC was probed at altitudes between 10.3 and 11.9 km (see Fig. S4). ECMWF winds at the 250 hPa model level, which corresponds approximately to the flight altitude, are shown in Fig. 1.

2.1 CARIBIC trace gas and aerosol measurements

The CARIBIC container houses a number of different instruments for measuring various trace gases as well as aerosol particles (Brenninkmeijer et al., 2007). Discussed extensively in this work are carbon monoxide (CO), ozone (O_3), the sum of reactive nitrogen oxides (NO_y) and aerosol particles (N_{4-12} and N_{12}). Brief descriptions of these measurements are presented next.

CO is measured with an AeroLaser AL 5002 resonance fluorescence UV instrument modified for use onboard the CARIBIC passenger aircraft. Alterations were necessary

to optimise the instrument reliability to allow for automated operation over an entire CARIBIC flight sequence lasting several days. The instrument has a precision of 1–2 ppbv at an integration time of 1 s and performs an in-flight calibration every 25 min. A technical description of the CO instrument can be found in Scharffe et al. (2012).

The ozone measurement is based on a fast, commercially available dry chemiluminescence (CL) instrument, which at typical ozone mixing ratios between 10 ppbv and 100 ppbv and a measurement frequency of 10 Hz has a precision of 0.3–1.0 %. The absolute ozone concentration is inferred from a UV-photometer designed in-house which operates at 0.25 Hz and reaches an accuracy of 0.5 ppbv. The CL instrument has been characterised in detail by Zahn et al. (2012).

The sum of reactive nitrogen oxides (NO_y) is detected using a two-channel NO monitor where chemiluminescence detection is used with NO_y being measured after catalytic conversion to NO (Ziereis et al., 2000). The time resolution is also 1 s. The overall uncertainty for the NO_y measurement at 10 s time resolution is about 7 % at 450 pptv NO_y (Brough et al., 2003).

The total water mixing ratio (gaseous, liquid and ice phase) is measured by means of a chilled mirror frost-point hygrometer (CR-2, Buck Research Instruments L.L.C.) with a time resolution of 5 (high humidity) to 300 s in the dry lowermost stratosphere with an uncertainty of around 0.3 ppmv at cruise altitude. A modified two-channel photoacoustic diode-laser spectrometer (Hilase, Hungary) measures both gaseous (H_2O_{gas}) and total water mixing ratios with a time resolution of 3 s and a precision of 1 ppmv. These measurements are calibrated to the absolute water mixing ratios determined with the frost-point hygrometer. A detailed description of the CARIBIC humidity measurements is available in Dyroff et al. (2014). An overview of the H_2O data has been published by Zahn et al. (2014).

Integral aerosol particle number concentrations are measured with three condensation particle counters (CPC, modified TSI model 7610) with lower threshold diameters (50 % counting efficiency) of 4, 12 and 18 nm, respectively, and an upper detection limit of around 2 µm at 200 hPa operating pressure (Hermann and Wiedensohler, 2001).

The difference of the 4 and 12 nm channels is called N_{4-12} and corresponds to the nucleation mode. The 12 nm channel (N_{12}) corresponds mainly to the Aitken mode in the upper troposphere where the CARIBIC aircraft is taking measurements. All aerosol particle number concentrations used in this paper are given at standard pressure and temperature (STP) of 273.15 K, 1013.25 hPa.

Whole air samples are collected in two units, each of which contains 14 glass sampling flasks of 2.7 L volume, pressurised to ~ 4.5 bar during collection. Samples were collected at pre-determined, evenly spaced intervals of roughly 35 min (~ 480 km) with filling times between 0.5 and 1.5 min (~7–22 km). In months with four flights between Frankfurt and Chennai, i.e. June, August and September 2008, sample collection only took place during the first two flights in order to achieve higher spatial and temporal resolution. Greenhouse gases and non-methane hydrocarbons (NMHCs) are measured post-flight in the laboratory at the Max Planck Institute for Chemistry in Mainz using separate gas chromatography (GC) systems coupling GC separation with flame ionisation detection (GC-FID) or electron capture detection (GC-ECD) (Schuck et al., 2009; Baker et al., 2010).

2.2 FLEXPART trajectory calculations

FLEXPART is a widely used Lagrangian particle dispersion model in ongoing development at the Norwegian Institute for Air Research (NILU) that in our case obtains its meteorological input data from the European Centre for Medium-Range Weather Forecasts (ECMWF). It simulates long-range and mesoscale transport, diffusion, dry and wet deposition, and radioactive decay of various tracers (see detailed description in Stohl et al., 2005). An updated description of the FLEXPART model is available from Stohl et al. (2010). In the current study, FLEXPART version 9.02 together with ECMWF meteorological input data with a temporal resolution of three hours and a spatial resolution of 1.0° × 1.0° and 91 model levels was used.

We started trajectories every 3 min along the flight tracks and calculated them 14 days forward and backward in the single trajectory mode of FLEXPART with enabled parameterisations for the sub-grid terrain effect and sub-grid convection. The trajectory positions were recorded every 30 min. The southernmost point of our flight track is Chennai (12.99° N, 80.18° E). The northern cut-offs for the trajectory analysis are 36.5° N in June, 40.0° N in July and August, and 35.5° N in September (see Table 1) and were chosen to exclude the subtropical jet stream and thus concentrate the analysis on the monsoon region. The continuous trace gas measurements were averaged over 60 s centred around the start points of the trajectories along the flight track to obtain representative trace gas concentrations for the air characterised by the trajectories.

3 Results and discussion

In the following, we first present the CARIBIC observations of trace gases and aerosol particles (Sect. 3.1.1) and their latitudinal and photochemical distributions and characteristics (Sect. 3.1.2) before investigating the vertical profiles measured by CARIBIC over Chennai in Sect. 3.1.3. Then we show the origins of these air masses (Sect. 3.2) and continue with a description of where the air is transported to after it has spent time in the monsoon upper troposphere anticyclone (UTAC) and how long it remains trapped inside the UTAC (Sect. 3.3).

3.1 CARIBIC observations

Here we present the CARIBIC observations and what the latitudinal and vertical variations in the trace gas mixing ratios tell us about the chemical properties of the air masses and their origin.

3.1.1 Position within the upper troposphere anticyclone

Along routes between Chennai and Frankfurt during the monsoon season (June–September 2008) the aircraft passed from the southern section of the UTAC, where

winds are from the east, through the centre into the northern section, where winds are from the west or vice versa for flights from Frankfurt to Chennai. The transition between the two regimes is evident in the wind data recorded by the aircraft, with an abrupt change in wind direction observed in the vicinity of 26° N (Fig. 2, note that 90° means wind from the east, 180° from the south, 270° from the west). Wind speeds are low in the centre of the UTAC, reaching near zero at the transition point and increasing strongly at the northern edge of the UTAC and upon entering the northern hemisphere subtropical jet stream. The latitude where the aircraft crosses between the two regimes varies from month to month, with the northernmost average location in July and the southernmost in September (Figs. 2, 3 and Table 1). There are also variations between flights in each month, with the point of transition on the flights to Chennai being further north than the corresponding return flights. This arises from the variations in flight altitude with flights to Chennai being at about 1–2 km higher altitude than the return flights at the transition point (see Fig. S4). The flight routes themselves, however, did not change between 22 and 30° N from month to month for the forward and return flights with the exception of one return flight in August (Fig. S5). Therefore changes between months at the same altitude reflect changes in monsoon circulation in the horizontal and/or the vertical direction. In general, the centre of the UTAC is observed to be furthest north during July, and this observation is consistent with meteorological studies of monsoon development, northward propagation and recession (IMD, 2014).

In an effort to compensate for biases attributable to variations in flight routes and/or horizontal movements of the monsoon UTAC, and to normalise for position within the UTAC between months, data are given an additional latitudinal coordinate. Relative latitude (Δlat) describes the location relative to the latitude at which the aircraft crosses from the northern to the southern section of the UTAC or vice versa (i.e. relative to the "centre" of the UTAC indicated by the reversal of the zonal wind). Positive Δlat describes measurements in the north, negative Δlat measurements in the south, with values determined on a per flight basis.

3.1.2 Latitudinal transects

As the aircraft moved from south to north we observed a distinct latitudinal structure in chemical tracers at altitudes of 10.3 to 11.9 km between approximately 15 and 40° N, shown in Fig. 4 for a single flight in August, when the UTAC was fully developed. The southern section of the flight track (12–28° N) is characterised by relatively low O_3 (panel A, mean concentrations over all flights and Δlat −7.5 to −2.5° of 51 vs. 81 ppb for Δlat 2.5 to 7.5°) and NO_y (panel B, mean concentrations of 0.56 vs. 0.81 ppb) and elevated CO (panel A, 101 vs. 92 ppb), water vapour (panel B, 390 vs. 35 ppm) and aerosol particles (panel C). In the north (28–40° N), the opposite is observed; mixing ratios of O_3 and NO_y are elevated, while levels of CO decrease and especially levels of water vapour and aerosol particle concentrations are much lower, with the exception of some brief instances of elevated nucleation mode (N_{4-12}) particle number concentrations. This distinct pattern is observed during all flights under investigation in all months and is attributable to the influence of different air mass source regions, different chemical regimes and varying transport times within the different regions of the UTAC (see Figs. 5 and S9–S24).

An important feature of the monsoon is persistent deep convection over South Asia, which is strongest over the Bay of Bengal and the Indian subcontinent (Devasthale and Fueglistaler, 2010). South of ∼ 25° N the aircraft encountered air that has passed over these highly active convective regions and has become burdened with emissions from South Asia. This accounts for enhancements in the primary pollutant CO and relatively low levels of the secondary pollutant O_3, as well as the enhancements in water vapour and nucleation mode aerosol particles (i.e. freshly formed particles, N_{4-12}), which can be regarded as tracers for convection (Weigelt et al., 2009) and are very short-lived relative to the other species (hours to a few days). Interestingly, mixing ratios of NO_y are lower in the south than in the north, possibly as a result of lower NO_x emissions in the south combined with the conversion to water soluble components of NO_y in the highly reactive polluted air masses followed by enhanced removal under the high

temperature, high humidity conditions of the monsoon. In the north, the air parcels encountered by CARIBIC have been transported for longer periods of time within the UTAC and show signs of chemical aging. Water vapour and nucleation mode particles have been depleted by experiencing cold temperatures during transport and washout, respectively. CO levels are reduced and O_3, given more time to form photochemically, is elevated. Similar changes in composition could have been caused by in-mixing of stratospheric air. However care has been taken to identify and remove all data points that have stratospheric influence based on the measured ozone concentrations and the potential vorticity (PV) values from the ECMWF model. The results are supported by our previous findings from measurements of NMHCs (Baker et al., 2011).

A comparison of the latitudinal profiles for the first return flight to Chennai during each month is shown in Fig. 5. Profiles for subsequent flights are shown in Figs. S22–S24. In general, trace gas (panels A–D) and aerosol particle (panels E and F) profiles in June, July and September are similar to those observed in August, although mixing ratios vary between the months, and in each month the overall pattern is interrupted by unique events. Notable features are the much higher NO_y (panel D) and lower CO (panel B) in the north during September, and the abrupt gradient in CO concentrations between north and south during June. The large variability in aerosol particles compared to the trace gases is caused by the strong dependency of the particle number concentration on clouds whose position relative to the CARIBIC flight tracks was different during each flight. Monthly mean particle distributions by latitude are shown in Sect. S5.

As our analysis focuses on the monsoon as a transport mechanism for polluted air masses from South Asia and Mainland Southeast Asia and the influence on other regions, understanding the composition and chemistry of air parcels as they move through the UTAC is critical in evaluating the potential impact on downwind regions. This includes understanding not only of primary pollutants in transported air masses, but also of the tendency to form secondary pollutants, in particular ozone. Previous analysis of the relationship between ozone and NMHCs, which are indicators of pollution and act as ozone precursors, has shown that air masses in the south have a

greater ozone formation potential than in the north, where air masses have diminished formation potential or show the beginnings of ozone destruction (Baker et al., 2011). Ozone formation potentials in the troposphere can also be qualitatively understood through the relationship between ozone and carbon monoxide using the enhancement ratio $\Delta O_3/\Delta CO$ (Fishman and Crutzen, 1978; Parrish et al., 1998; Zahn et al., 2002), as determined from correlation plots, in addition to the information provided by the coarser resolution NMHC data. Positive slopes of the correlation, i.e. $\Delta O_3/\Delta CO > 0$, indicate the formation of ozone. Negative correlations can (outside of stratospheric influence) indicate destruction of ozone or in-mixing of different air masses, which may also apply when a lack of correlation is observed (Parrish et al., 1993; Trainer et al., 2000; Voulgarakis et al., 2011, and references therein).

Figure 6 shows O_3 vs. CO during each of the four monsoon months with colour-coding indicating relative latitude. For all months, the slope $\Delta O_3/\Delta CO$ changes from positive at the southernmost latitudes to negative at the northern edge of the UTAC ($\Delta lat \sim 15^{\circ}$). August is the month with the clearest latitudinal pattern in the slope $\Delta O_3/\Delta CO$: strong, positive relationships are observed in the south and immediately north of the transition point (0° Δlat), and negative correlations are found in the far north. Patterns in other months show some characteristics of the relationships observed in August, for example, positive correlations in the south in June and July and negative correlations in the north in all months. These relationships provide an indication that ozone forming regimes dominate in the south and also immediately north of the transition point, while in the northern part of the UTAC there is no clear potential for ozone formation (see also Sect. S6 and Fig. S28). Ambiguous relationships near the transition point are most likely related to this region being most strongly and recently affected by continental emissions and/or air masses influenced by mixing during their transport, resulting in a broader range of air mass ages or sources. All these tendencies are determined from the slope of $\Delta O_3/\Delta CO$ over a few degrees latitude which agrees with the range of 200–500 km used in an earlier study by Zahn et al. (2002, their Fig. 10). The correlations for the individual flights (not shown) yield similar qualitative

results as expected since the time between the individual flights through the monsoon in one month is short (12–36 h) compared to the transport time of the air inside the UTAC (many days).

3.1.3 Vertical profiles over Chennai

The majority of flight time through the UTAC was spent at cruise altitude in a narrow altitude range, between 10.3 and 11.9 km (see Fig. S4), providing limited insight into the vertical distribution of trace species in the UTAC along the flight route. However, the descent into and take-off from Chennai airport provide us with some information in the vertical in the southern part of the UTAC, as the aircraft passes between ∼ 11 km and ground level over a relatively short distance (∼ 200–250 km) in approximately 30 min (Fig. S4). During this time the aircraft moves from being within the UTAC into the free troposphere below and eventually into the boundary layer and vice versa. In situ data are available for most species down to ∼ 2 km, with the exception of water vapour which is available down to ∼ 5 km only and NO_y, which is not available below ∼ 10 km for these flights. Aerosol concentrations during ascent are only available above 6 km because the CPCs need some time before they are ready to start the measurements. No whole air samples were collected on ascent and descent. Both ascent and descent took place during night, with landing times around 23:30 LT (local time) and take-off between 02:00 LT and 03:40 LT the following morning (Fig. S4). Descents into the airport were from a west–north-west direction towards the Bay of Bengal and final approaches from the east while the ascents were over land west of Chennai (except for the September flights which took off to the east). Similar flight times and patterns were followed for all flights except for July where the approach into Chennai followed a route further north of Chennai before the final approach to the airport from the east (see Fig. S6).

While descending from cruise altitude, the aircraft moved from the westward flow of the UTAC into the eastward flow of the low level Somali Jet. This is clearly visible in the wind direction measured by the CARIBIC aircraft shown in Fig. 7. In June and

August this transition occurred between 6 and 7 km, while in September it was around 9 km altitude. In July, tropospheric wind speeds were much lower than in the other months and there was no wind reversal evident from the measurements. This was a general feature of the meteorology on 15 and 16 July when the flights took place. Over a large region in Southeast India and out over the adjacent Bay of Bengal, wind speeds were very low from the surface up to 500 hPa (∼ 5 km) which is about the height of the wind reversal seen in Fig. 7 in June and August. The corresponding ECMWF wind fields during the days of the flights are shown in Fig. S7 (745 hPa winds) and Fig. S8 (510 hPa winds). Over Central India and the Indian Ocean south of India there were eastward winds extending the Somali Jet over the Indian subcontinent and into the Bay of Bengal. But just around Chennai, winds were very calm. This has probably led to a trapping of the local pollution from the city of Chennai during these days in July 2008, whereas higher wind speeds in the lower troposphere were encountered in the other months.

Vertical trace gas and aerosol particle profiles during descent and ascent show a fairly consistent picture during the monsoon season, with the exception of July (see Fig. 8). Trace gas data for the two July flights reflect the unique meteorological situation described above, particularly during the descent into Chennai, which was very dry and had strongly enhanced O_3 (panel B) which increased with decreasing altitude and reached 116 ppb at the lowermost point (not shown). These profiles were also characterised by high CO (panel A) between 6 and 9 km, which is above the level of wind direction change. There was no recognisable change in the number concentration of Aitken mode aerosol particles (panel D). In the free troposphere there was a weak north-westward flow (see Fig. 7) which would transport the pollution of Chennai and its industrial sources right to the region where the July flight descended into Chennai airport (see Fig. S6) while the other flights descended from the west–north-west, i.e. mostly upstream of the pollution sources in Chennai.

In the other months, the vertical "C"-shaped profiles of CO (see Fig. 8a) reflect the position change outside and inside of the UTAC as the aircraft ascends into the upper

troposphere. Moving upward from 2 km, mixing ratios of CO decrease until reaching the point where the wind direction changes, marking entry into the lower levels of the UTAC. Here, CO begins to increase, often reaching, and even exceeding, maxima observed at lower altitudes. The difference between maximum and minimum is most pronounced in June with mixing ratios in the middle troposphere being higher than in the other months, when mixing ratios are fairly similar. No significant differences between ascents and descents are observed.

Profiles of O_3 (Fig. 8b) show increasing mixing ratios with altitude, with no clear transition between free troposphere and UTAC and no significant differences between ascent and descent. A monthly trend is present, with the lowest values in August and the highest values in June, when the vertical gradient was also steepest. Monthly differences are most pronounced above 6 km. Conversely, water vapour (Fig. 8c, note logarithmic scale on *x* axis) decreased with altitude, with a similar vertical gradient during each month. June profiles were the driest, with the exception of the second flight into Chennai in September and the flight into Chennai in July (see above). June is at the beginning of the monsoon season in India when precipitation is not yet as high as during the following monsoon months.

Concentrations of the Aitken mode aerosol particles (N_{12}, Fig. 8d, logarithmic scale on *x* axis) show a positive vertical gradient, except for one descent in August which is variable with altitude but shows no consistent trend. There are no significant monthly differences in concentration or gradient. Also N_{12} particle number concentrations during ascent and descent are more or less equal considering their general variability with altitude. This is expected since both descent and take-off in Chennai occur many hours after nightfall when all direct influence from the daytime convective activity has ceased. Part of the variability of the vertical N_{12} profiles is due to crossing of contrails of other aircrafts with locally very high aerosol particle number concentrations.

Measurements of O_3 profiles with MOZAIC (Measurement of OZone by Airbus In-service airCraft) aircraft over Chennai in 1996 and 1997 (Sahu et al., 2011) and Hyderabad in central India in 2006–2008 (Sahu et al., 2014) showed similar concentrations

and a similar positive gradient with altitude. However, none of these observations documented a large increase towards the surface in the monsoon months as observed by CARIBIC in July 2008. MOZAIC CO profiles measured over Hyderabad in 2006–2008 (Sheel et al., 2014) were more or less constant at ∼ 100 ppb throughout the free and upper troposphere and only showed an increase towards the surface below ∼ 4 km. A pronounced increase of CO in the free troposphere as measured by CARIBIC in July 2008 has not been observed over Hyderabad in the summer months of these years. This corroborates that 15/16 July 2008 was an exceptional case with respect to the CO and O_3 profiles over Chennai.

3.2 Source regions of monsoon air

The focus of this study is on the export of polluted air masses from the UTAC, in other words how and where "leaks" from the UTAC occur and how this might influence long-distance pollution transport in the northern hemisphere. However, it is also of interest to investigate its origin and subsequent processing during the trapping in the UTAC at low temperatures, pressures and water vapour under high insolation. In previous CARIBIC papers we have discussed the issue of the origin of certain pollutants (Schuck et al., 2010; Baker et al., 2011, 2012). Figure 9 shows trajectories calculated with the FLEXPART model for a representative case to identify the origin of the air that was sampled by the CARIBIC aircraft when flying through the UTAC. The backward trajectories for the CARIBIC flight to Chennai on 13 August 2008 are colour-coded with trajectory altitude in kilometres above sea-level (km a.s.l.). As the trajectory reliability decreases with time into the past (and future), we used only the first 10 days for the source and receptor region analysis and in all subsequent plots.

For the northern part of the flight track the observed air masses, approaching from the west, have resided for many days inside the UTAC at altitudes (indicated by the trajectory colour in Fig. 9) at or above the CARIBIC flight altitude. In the southern part, the air masses reached the CARIBIC flight track from the east after having been convected from the lower troposphere into the upper troposphere over or east of the

Bay of Bengal originally having followed an eastward flow with the Somali Jet over the Arabian Sea and Central and Southern India. Only when approaching Chennai airport at low altitudes we observed air coming directly from the west without having passed over the Bay of Bengal.

A summary of the source regions for the air masses sampled by CARIBIC during the August 2008 flights is shown in Fig. 10. It shows the geographical distribution of where the backward trajectories (starting at flight altitude) first descended below 5 km altitude. The upper panel shows the source region distribution for the trajectories starting north of the wind reversal; the lower panel shows the source region for CARIBIC observations in the southern part of the UTAC. For the northern part of the UTAC, the air came from Eastern India, the Indo-Gangetic-Plain as well as from the northern parts of the Bay of Bengal, Mainland Southeast Asia and the South China Sea. The air measured by CARIBIC in the southern part of the UTAC originated in central and southern India, the Bay of Bengal and the western part of Mainland Southeast Asia. Apart from the contribution of Mainland Southeast Asia and the South China Sea, the source regions for the northern and southern part of the UTAC did not differ significantly. While the general pattern was similar for the other flights in June–August 2008, the exact location of the convective uplift and hence the source regions varied and were more widely distributed than during August (see Figs. S29–S31).

3.3 Outflow from the UTAC

The following subsections describe the fate of the air and the contained trace species observed with CARIBIC after they have been processed in the monsoon UTAC. This includes to which regions they are transported to based on the FLEXPART trajectories and how long they have resided in the UTAC.

3.3.1 Receptor regions of monsoon air

FLEXPART forward trajectories were used to determine to where the air and the trace species, observed by CARIBIC at cruise altitude in the South Asian monsoon UTAC, were transported and by this revealing which regions were directly influenced by the outflow of the polluted air masses (Schuck et al., 2010; Baker et al., 2011). We defined seven receptor regions, listed in Table 2: North America, Central Pacific, Central Africa and the Mediterranean over which we defined boxes reaching from the ground to the thermal tropopause. The trajectories are detected over these regions if they are within the defined boxes using the local thermal tropopause height output from the FLEXPART model along the trajectories. The South Asian monsoon region is defined as an ellipse with the centre at 80° E longitude while its latitude is between 22.7–27.9° N depending on the actual flight (see last column in Table 1). The monsoon centre latitude is determined from the zonal (west–east) wind reversal along the flight track using the wind speed and direction measured during flight by the aircraft (see Sect. 3.1.1). To qualify as a monsoon trajectory, the trajectory has to stay for at least 70 % of the 10 day period within the monsoon ellipse and below the thermal tropopause. Trajectories which stayed for at least 24 h above the thermal or dynamical tropopause (PV > 2.5 PVU) were counted as TP (tropopause) or PV stratospheric trajectories, respectively. As expected, all but one of the trajectories which met the criterion for the dynamical tropopause also met the criterion for the thermal tropopause.

As each forward trajectory may cross several receptor regions, we determined the fraction of time the trajectory stayed inside each receptor region from the number of 30 min trajectory time-steps that were inside the receptor region. An example for this analysis is shown in Fig. 11 for the flight on 13 August 2008 where the flight track is shown by the thick red line. Each panel shows all the forward trajectories (south of the northern cut-off) for this flight in grey. The trajectories which cross the different receptor regions are shown in red (North America), magenta (Central Pacific), green (Central Africa), blue (the Mediterranean), and orange (South Asian monsoon). The lower-

most right panel shows the trajectories with stratospheric parts in yellow (for thermal tropopause criterion) and pink (dynamical tropopause criterion). As mentioned above, the dynamical tropopause usually is somewhat higher than the thermal tropopause. Therefore the pink trajectories form a subset of the yellow trajectories except for one trajectory which is classified as stratospheric according to the dynamical tropopause but not according to the thermal tropopause.

The aggregate results for the receptor region analysis based on the forward trajectories are shown in Fig. 12. It shows the percentages of trajectories reaching the seven receptor regions defined in Table 2 averaged for each month between June and September 2008. Since a trajectory may reach more than one receptor region (e.g. Central Africa and Mediterranean, Central Pacific and North America, or dynamical PV stratosphere and thermal TP stratosphere), the totals exceed 100 %. The least receptor region overlap is observed in September (the total is closest to 100 %) while the trajectories in July reach the largest number of receptor regions. July is also different from the other months in that it has the largest fraction of outflow to the west, i.e. to Central Africa (green bar) and further on to the Mediterranean (blue bar). This may be a peculiarity on 15/16 July 2008 when the flights took place. Note that in July there were only two flights and not four as in the other months.

The latitudinal distribution of the receptor regions (not shown) for the air sampled by the CARIBIC aircraft varies from flight to flight but the general tendency is that air sampled in the north is mostly either exported towards the east or entering the stratosphere while most air masses that are exported towards Africa and the Mediterranean have been sampled in the southern part of the flight track through the UTAC. Interestingly, air sampled in the middle of the UTAC, i.e. at the location of the wind reversal, and a few degrees south appears to have the highest likelihood of being transported to the stratosphere. In September, the transport is somewhat different, with less air sampled in the middle of the UTAC moving to the stratosphere but instead more air remains in the UTAC and the region where air is exported towards the east is expanding southwards. This shift in the latitudinal distribution may be the result of a weakening monsoon cir-

culation towards the end of the monsoon season. The actual monsoon withdrawal as diagnosed by the India Meteorological Department however started in 2008 at the end of September (IMD, 2014).

3.3.2 Estimating transport times

An important cross-check of the FLEXPART trajectory calculations is possible by comparing with the photochemical age of air pollutants estimated from ratios of NMHCs measured in the whole air samples collected in July and August 2008. The photochemical age is used as a proxy for the time since the pollutants had been emitted into the air mass. Details of the NMHC age calculation have been published previously by Baker et al. (2011). For samples collected south of the wind reversal, that had recently convectively been lifted to cruise altitude, an estimated mean OH concentration $\langle[OH]\rangle$ of 2.48×10^6 molecules cm^{-3} (Spivakovsky et al., 2000) and emission ratios of 0.29 and 0.15 for propane/ethane and n-butane/ethane, respectively, were used. For air samples collected north of the wind reversal, which had resided for a longer time inside the UTAC, we instead applied an estimated $\langle[OH]\rangle$ of 1.44×10^6 molecules cm^{-3} (Spivakovsky et al., 2000). Figure 13 shows a clustering of the NMHC ages, with photochemically younger air in the south (Δlat $<\sim 3^\circ$) which had recent contact with fresh emissions and older air in the north with more aged air having already experienced several days of photochemical processing during transport in the UTAC. For each air sample Fig. 13 shows the mean photochemical age of the air sample together with the minimum and maximum age determined from the propane/ethane, n-butane/ethane and n-butane/propane ratios.

The comparison of the chemical age of the air pollutants with the transport times estimated from the FLEXPART trajectory calculations is shown in Fig. 14. The best fit was found when comparing the time since the air had last been east of 90–95° E (Fig. 14 shows the time since the air was last east of 95° E). The linear least-squares regression lines have slopes of 0.98 and 0.93 and Pearson correlation coefficients R^2 of 0.87 and 0.68 for the flights in July and August, respectively. Considering that the

NMHC age uses surface emission ratios estimated from ground-based data as the starting point for the age calculations and that convection (which is partly parameterised in the FLEXPART model) is most frequent over the Bay of Bengal, a source region east of 90–95° E seems reasonable and fits to the source regions discussed in Sect. 3.2. Approximate overall agreement between the two methods provides confidence that our interpretation of pollutant distributions and transport within the UTAC is realistic. In most cases where there is a large disagreement between NMHC chemical age and FLEXPART transport age, the NMHC ages show a large spread. Reasons for this may be mixing with background air containing NMHCs, different source ratios than assumed in the analysis or situations where the OH concentrations deviated from the assumed climatological averages used in the NMHC age calculations. Uncertainties of ⟨[OH]⟩ of ±25 % correspond to uncertainties of the derived NMHC ages of 20–33 % (see Baker et al., 2011).

3.3.3 Monsoon UTAC "leak" rates

The South Asian summer monsoon UTAC is often described as a processing reactor for the pollution emitted at the surface which is transported upward by convection and then trapped in the UTAC (e.g. Park et al., 2008; Schuck et al., 2010; Randel and Jensen, 2013, and references therein). However, the horizontal wind fields shown in Fig. 1 and the forward trajectories in Fig. 11 indicate that the trapping is temporary. At the south-western part of the UTAC, some air escapes to Central Africa, part of which may return via the Mediterranean and the Middle East to become again entrained in the UTAC in the northwest. In the northeastern region, air is leaving the UTAC with the eastward jet stream and is transported over China towards the Pacific and finally Northern America. Quantifying this loss is the goal of the leak rate analysis described below.

The calculated trajectories have been used to estimate the residence time of the observed air inside the monsoon ellipse defined above. For this analysis, only the trajectories along the flight track that start inside the ellipse are used. The number of

trajectories remaining within the ellipse was determined for the preceding and following 10 days at time steps of 6 h centred around the middle of the time period the flight track spent inside the ellipse, i.e. the middle from the aircraft entering the ellipse at its northern edge and the touch-down at Chennai and vice versa for southward and northbound flights, respectively. This analysis is similar to leak rates calculated by Randel and Park (2006, their Fig. 14).

The results, colour-coded for flight month, are shown in Fig. 15. The solid coloured lines show the monthly means while the dashed black line indicates the average over all months. On average, 65 % of the trajectories had resided inside the ellipse for at least 10 days while 30 % of the air was entrained within the last three days prior to the measurements. Following the air masses after the measurement shows a different picture: after 6 days only 50 % of the trajectories, on average, are still within the ellipse. However, while fewer trajectories were within the ellipse before the measurement in August, they tended to remain inside longer after the measurement than in the other months. Especially in June and September, the exit from the ellipse was more rapid than in July and August, related to the weaker monsoon circulation during these months. The calculated leak rates are higher, i.e. the trajectories leave the trajectory faster, than those calculated by (Randel and Park, 2006) which is consistent with the much larger monsoon anticyclone area definition used by these authors.

An explanation for the asymmetric shape of the calculated leak rates could be related to the position of the aircraft within the UTAC and hence within the monsoon ellipse defined above. The flight tracks cross the western part of the ellipse. The UTAC has two main points of air discharge: one in the south-west where air is transported westwards towards Africa and one in the north-east where it is transported eastwards towards China and the Pacific Ocean. In the northern part of our flight track inside the UTAC, the air masses observed had not left towards Africa but stayed inside the UTAC. In the forward direction, the air masses have a chance of leaving the UTAC at its north-eastern part, i.e. towards China and the Pacific Ocean. Having traversed to the southern part, the air masses observed have not left towards the Pacific but stayed

inside the UTAC. But looking forward again, the air masses have a chance of leaving the UTAC towards Africa. Since the calculated leak rates are an average over all trajectories started inside the UTAC, the tendency that the air masses have already been for quite some time inside the UTAC (at least the majority of the trajectories) while looking forwards, the air masses have a higher chance of leaving the UTAC quickly (or at least faster than they have entered the UTAC) seems to be consistent with our understanding of the monsoon circulation. In August, which from all CARIBIC data seems to be the most representative monsoon month (red lines in Fig. 15), the UTAC contains the air masses more strongly than in the other months. In addition, Figs. S32 and S33 show that the trapping efficiency is comparable even when considering altitudes that are 2 km above the actual flight altitudes. This is somewhat unexpected. As the UTAC has its maximum some kilometres above the actual flight altitude of the CARIBIC aircraft of ∼ 11–12 km (Park et al., 2008), an even stronger confinement at altitudes above the CARIBIC flight altitudes would be expected.

4 Conclusions

The data from the CARIBIC passenger aircraft observatory discussed in this study cover the South Asian summer monsoon season 2008 from June to September. The flights largely crossed the western part of the summer monsoon UTAC at an altitude of ∼ 11 km which is believed to be at its bottom part where pollution levels are possibly lower than a few kilometres aloft where the UTAC is even stronger (e.g. Park et al., 2008). Figure 6, however, showing tracer-tracer correlations over a distance of 3500 km (approximately from Teheran, Iran to Chennai, India), demonstrates the extent of the UTAC and the remarkable consistency of the CARIBIC observations, where trace gas distributions show regular patterns during monthly flights and even from month to month (previously reported by Schuck et al. (2010) and Baker et al., 2011). Earlier observations from CARIBIC phase 1 in the summers 1998–2000, despite consisting of a more limited chemical dataset (Hermann et al. (2003); Zahn et al. (2002) and unpub-

lished data), also consistently show a similar development of the monsoon in terms of trace gas and aerosol particle distributions during flights from Germany to Colombo, Sri Lanka and Male, Maldives (not shown). These results will be published separately but underscore that the present dataset is representative even though it consists of a few flights per month only.

In accordance with our current understanding of the South Asian summer monsoon and in particular its role trapping surface air that was rapidly transported upwards by convective activity, all the CARIBIC observations during the monsoon months in this region, although they were made in different years, fit the same overall picture of pollution build-up in the UTAC. Starting from this consistent dataset, of particular interest is on the one hand the understanding of the chemical composition of the air in the UTAC and on the other hand the export of this air to other regions, for which the CARIBIC flight to Toronto in September 2007 (see Sect. S1) gives a good example.

Based on the measured reversal of the zonal wind at flight altitude across the centre of the UTAC located at 27° N in June to 23° N in September (Table 1, cf. New Delhi 28.4° N, Calcutta 22.3° N), the chemical and aerosol particle data are presented using relative latitude with respect to the wind reversal and by doing so provide a very consistent picture of humid, recently polluted, low O_3, medium CO air and low NO_y air with a high burden of aerosol particles in the south and a strengthening tendency (increasing CO and O_3, declining humidity) towards the centre of the UTAC. Northwards from there dry air, with higher NO_y, but strongly declining CO, moderately declining O_3 (up to a relative latitude Δlat of around 12°) and low aerosol particle number concentrations is observed.

The vertical profiles of O_3 and CO over Chennai are very distinct compared to other profile observations over India (cf. Sheel et al. (2014); Sahu et al. 2014). They are likely influenced by the local emissions in the Chennai area together with the advection of clean maritime air and polluted air from other parts of India and the surrounding region to form the characteristic "C"-shape observed for CO in all months except July. In that month a strong free tropospheric CO enhancement of up to 116 ppb was observed

which cannot be explained solely by local convection of polluted surface air but is instead probably due to long-range transport of polluted air masses. Detailed modelling studies to understand these vertical profiles are currently ongoing and will be published separately (Ojha et al., 2015).

Hydrocarbon ratios used in photochemical age of air calculations show that the air masses in the southern part of the UTAC are younger (chemical ages between 3.5 and 6.5 days) than in the north (chemical ages between 10 and 13.5 days). The clustering of the chemical ages compares well with that based on the transport age determined from the FLEXPART backward trajectories, namely 1–7 days compared to 7–14 days for transport from 95° E to the CARIBIC flight track. The spread in the FLEXPART transport ages is larger and they are in general higher by 0.5–1.5 days. Given the uncertainties of air mass trajectory calculations, the problems in how to determine its starting point in time over polluting sources and given the uncertainty in photochemical age that may be affected by dilution with background air, the correspondence is encouraging.

Air sampled by CARIBIC originated from a large region. Although the convection over the Bay of Bengal is greatest, for a quantification of its effect on pollution the vertical transport has to be combined with the emission source distributions which is beyond this study (see Ojha et al., 2015). Instead we have focused on the FLEXPART backward trajectory based footprint (air at cruise level that had come from below 5 km) for air in the southern and northern part of the UTAC. For the southern part, the footprint is situated somewhat more to the west. For August the surface area of the footprint is largest (Fig. 10). When the UTAC wanes in September, and its centre moves south to reach 23° N north, the footprint likewise shifts southward. However, no major differences in footprint for air in the southern compared to the northern part of the UTAC exists; the age difference seems to be the fundamental difference.

The receptor region analyses and the "leak" rates show that air in the southern part of the UTAC is mostly in an ozone forming chemical regime (Fig. 6) and part of it is exported towards Central Africa and the Mediterranean. In contrast, the air in the north-

ern part, which features an ozone neutral or partially even ozone destroying chemical regime, is exported towards China and the Pacific ocean and in rare cases even up to the east coast of North America (Sect. S1). Export from the UTAC into the stratosphere peaked in June and July (Fig. 12). With CO values declining from June onward, this implies an "optimal" input of CO into the lowermost stratosphere. However, around two thirds of the air is dispersed within the troposphere. Such transport to the stratosphere has been observed in a similar way by the German HALO (High Altitude and LOng range) research aircraft, which detected monsoon pollution transported to the lowermost stratosphere over Europe in late summer 2012 during the TACTS (Transport And Composition in the upper troposphere/lowermost stratosphere) campaign (Roiger, 2014).

The large scale movement in the UTAC as in a large scale atmospheric "merry-go-around" is not without losses (Fig. 15). While surface air very high in pollutants reaches the UTAC from below and becomes trapped, similar amounts of air leak out of the system, mostly at its northeastern and southwestern edges. Still the trapping process is impressive. Even going back in time 10 days prior to sampling by CARIBIC, on average 65 % of the back trajectories had resided within the UTAC defined for this calculation as an ellipse. After having been probed by CARIBIC, only 40 % of the trajectories stay in the UTAC ellipse for more than 10 days. This asymmetry is an artifact of the geographical skew in the sampling by CARIBIC. Interestingly, calculations show that the leakage rates 2 km above cruise altitude of CARIBIC are not significantly lower (Sect. S8). A mass balance of the UTAC is beyond the scope of this work. No doubt, also air from outside the UTAC is being entrained, leading to dilution that intensifies towards it borders.

In the monsoon source region of South Asia lived about 1.4 billion people in 2008 (linearly interpolated to the year 2008 from Center for International Earth Science Information Network (CIESIN) data for 2000 and estimates for 2010) and the population is still growing. Together with the economic development in this region, this means that the pollutant emissions today are larger than in 2008 and will further increase in the

future. This also encompasses export of even more polluted air as shown in this study with implications for the atmospheric chemistry and air quality in the receiving regions.

The Supplement related to this article is available online at doi:10.5194/acpd-15-6967-2015-supplement.

Acknowledgements. We wish to thank all CARIBIC partners as well as Lufthansa, especially T. Dauer and A. Waibel, and Lufthansa Technik for their ongoing support for many years. We especially acknowledge D. Scharffe, C. Koeppel and S. Weber for the operation of this complex platform. The FLEXPART model has been provided by A. Stohl at the Norwegian Institute for Air Research (NILU) and was used with meteorological data from the European Centre for Medium-Range Weather Forecasts (ECMWF).

The article processing charges for this open-access publication have been covered by the Max Planck Society.

References

Assonov, S. S., Brenninkmeijer, C. A. M., Schuck, T. J., and Taylor, P.: Analysis of ^{13}C and ^{18}O isotope data of CO_2 in CARIBIC aircraft samples as tracers of upper troposphere/lower stratosphere mixing and the global carbon cycle, Atmos. Chem. Phys., 10, 8575–8599, doi:10.5194/acp-10-8575-2010, 2010. 6972

Baker, A. K., Slemr, F., and Brenninkmeijer, C. A. M.: Analysis of non-methane hydrocarbons in air samples collected aboard the CARIBIC passenger aircraft, Atmos. Meas. Tech., 3, 311–321, doi:10.5194/amt-3-311-2010, 2010. 6973, 6975

Baker, A. K., Schuck, T. J., Slemr, F., van Velthoven, P., Zahn, A., and Brenninkmeijer, C. A. M.: Characterization of non-methane hydrocarbons in Asian summer monsoon outflow observed by the CARIBIC aircraft, Atmos. Chem. Phys., 11, 503–518, doi:10.5194/acp-11-503-2011, 2011. 6971, 6973, 6979, 6980, 6984, 6986, 6988, 6989

Baker, A. K., Schuck, T. J., Brenninkmeijer, C. A. M., Rauthe-Schöch, A., Slemr, F., van Velthoven, P. F. J., and Lelieveld, J.: Estimating the contribution of monsoon-related biogenic

production to methane emissions from South Asia using CARIBIC observations, Geophys. Res. Lett., 10, L10813, doi:10.1029/2012GL051756, 2012. 6971, 6984

Brenninkmeijer, C. A. M., Crutzen, P., Boumard, F., Dauer, T., Dix, B., Ebinghaus, R., Filippi, D., Fischer, H., Franke, H., Frieß, U., Heintzenberg, J., Helleis, F., Hermann, M., Kock, H. H., Koeppel, C., Lelieveld, J., Leuenberger, M., Martinsson, B. G., Miemczyk, S., Moret, H. P., Nguyen, H. N., Nyfeler, P., Oram, D., O'Sullivan, D., Penkett, S., Platt, U., Pupek, M., Ramonet, M., Randa, B., Reichelt, M., Rhee, T. S., Rohwer, J., Rosenfeld, K., Scharffe, D., Schlager, H., Schumann, U., Slemr, F., Sprung, D., Stock, P., Thaler, R., Valentino, F., van Velthoven, P., Waibel, A., Wandel, A., Waschitschek, K., Wiedensohler, A., Xueref-Remy, I., Zahn, A., Zech, U., and Ziereis, H.: Civil aircraft for the regular investigation of the atmosphere based on an instrumented container: The new CARIBIC system, Atmos. Chem. Phys., 7, 4953–4976, doi:10.5194/acp-7-4953-2007, 2007. 6971, 6973

Brough, N., Reeves, C. E., Penkett, S. A., Stewart, D. J., Dewey, K., Kent, J., Barjat, H., Monks, P. S., Ziereis, H., Stock, P., Huntrieser, H., , and Schlager, H.: Intercomparison of aircraft instruments on board the C-130 and Falcon 20 over southern Germany during EXPORT 2000, Atmos. Chem. Phys., 3, 2127–2138, doi:10.5194/acp-3-2127-2003, 2003. 6974

Center for International Earth Science Information Network (CIESIN)/Columbia University: National aggregates of geospatial data collection: Population, Landscape, And Climate Estimates, Version 3 (PLACE III), NASA Socioeconomic Data and Applications Center (SEDAC), Palisades, NY, USA, available online at: http://sedac.ciesin.columbia.edu/data/set/nagdc-population-landscape-climate-estimates-v3, last access: 6 February 2015, 2012. 6994

Chen, B., Xu, X. D., Yang, S., and Zhao, T. L.: Climatological perspectives of air transport from atmospheric boundary layer to tropopause layer over Asian monsoon regions during boreal summer inferred from Lagrangian approach, Atmos. Chem. Phys., 12, 5827–5839, doi:10.5194/acp-12-5827-2012, 2012. 6971

Crawford, J. and Pan, L.: Atmospheric composition and the Asian monsoon: Results from a side meeting at the 12th IGAC Science Conference in Beijing, 17–21 September 2012, SPARC Newsletter, 40, 67, 2013. 6971

Devasthale, A. and Fueglistaler, S.: A climatological perspective of deep convection penetrating the TTL during the Indian summer monsoon from the AVHRR and MODIS instruments, Atmos. Chem. Phys., 10, 4573–4582, doi:10.5194/acp-10-4573-2010, 2010. 6978

Dyroff, C., Zahn, A., Christner, E., Forbes, R., Tompkins, A. M., and van Velthoven, P. F. J.: Comparison of ECMWF analysis and forecast humidity data to CARIBIC upper troposphere and lower stratosphere observations, Quart. J. Roy. Meteorol. Soc., doi:10.1002/qj.2400, 2014, published online. 6974

Fairlie, T. D., Vernier, J.-P., Natarajan, M., and Bedka, K. M.: Dispersion of the Nabro volcanic plume and its relation to the Asian summer monsoon, Atmos. Chem. Phys., 14, 7045–7057, doi:10.5194/acp-14-7045-2014, 2014. 6970

Fishman, J. and Crutzen, P. J.: The origin of ozone in the troposphere, Nature, 274, 855–858, doi:10.1038/274855a0, 1978. 6980

Garny, H. and Randel, W. J.: Dynamic variability of the Asian monsoon anticyclone observed in potential vorticity and correlations with tracer distributions, J. Geophys. Res., 118, 13421–13433, doi:10.1002/2013JD020908, 2013. 6970

Hermann, M. and Wiedensohler, A.: Counting efficiency of condensation particle counters at low-pressures with illustrative data from the upper troposphere, J. Aerosol Sci., 32, 975–991, doi:10.1016/S0021-8502(01)00037-4, 2001. 6974

Hermann, M., Heintzenberg, J., Wiedensohler, A., Zahn, A., Heinrich, G., and Brenninkmeijer, C. A. M.: Meridional distributions of aerosol particle number concentrations in the upper troposphere and lower stratosphere obtained by Civil Aircraft for Regular Investigation of the Atmosphere Based on an Instrument Container (CARIBIC) flights, J. Geophys. Res., 108, 4114, doi:10.1029/2001JD001077, 2003. 6971, 6991

IMD: India Meteorological Department: Monsoon website, available at: http://www.imd.gov.in/section/nhac/dynamic/Monsoon_frame.htm, last access: 6 February 2015, 2014. 6977, 6988

Kar, J., Bremer, H., Drummond, J. R., Rochon, Y. J., Jones, D. B. A., Nichitiu, F., Zou, J., Liu, J., Gille, J. C., Edwards, D. P., Deeter, M. N., Francis, G., Ziskin, D., and Warner, J.: Evidence of vertical transport of carbon monoxide from Measurements of Pollution in the Troposphere (MOPITT), Geophys. Res. Lett., 31, L23105, doi:10.1029/2004GL021128, 2004. 6970

Lawrence, M. G. and Lelieveld, J.: Atmospheric pollutant outflow from southern Asia: a review, Atmos. Chem. Phys., 10, 11017–11096, doi:10.5194/acp-10-11017-2010, 2010. 6971

Lelieveld, J., Berresheim, H., Borrmann, S., Crutzen, P. J., Dentener, F. J., Fischer, H., Feichter, J., Flatau, P. J., Heland, J., Holzinger, R., Korrmann, R., Lawrence, M. G., Levin, Z., Markowicz, K. M., Mihalopoulos, N., Minikin, A., Ramanathan, V., de Reus, M., Roelofs, G. J., Scheeren, H. A., Sciare, J., Schlager, H., Schultz, M., Siegmund, P., Steil, B., Stephanou, E. G., Stier, P., Traub, M., Warneke, C., Williams, J., and Ziereis, H.: Global air pollution

crossroads over the Mediterranean, Science, 298, 794–799, doi:10.1126/science.1075457, 2002. 6970

Lelieveld, J., Brühl, C., Jöckel, P., Steil, B., Crutzen, P. J., Fischer, H., Giorgetta, M. A., Hoor, P., Lawrence, M. G., Sausen, R., and Tost, H.: Stratospheric dryness: model simulations and satellite observations, Atmos. Chem. Phys., 7, 1313–1332, doi:10.5194/acp-7-1313-2007, 2007. 6970

Li, Q., Jacob, D. J., Logan, J. A., Bey, I., Yantosca, R. M., Liu, H., Martin, R. V., Fiore, A. M., Field, B. D., Duncan, B. N., and Thouret, V.: A tropospheric ozone maximum over the Middle East, Geophys. Res. Lett., 28, 3235–3238, doi:10.1029/2001GL013134, 2001. 6970

Liang, Q., Jaeglé, L., Hudman, R. C., Turquety, S., Jacob, D. J., Avery, M. A., Browell, E. V., Sachse, G. W., Blake, D. R., Brune, W., Ren, X., Cohen, R. C., Dibb, J. E., Fried, A., Fuelberg, H., Porter, M., Heikes, B. G., Huey, G., Singh, H. B., and Wennberg, P. O.: Summertime influence of Asian pollution in the free troposphere over North America, J. Geophys. Res., 112, D12S11, doi:10.1029/2006JD007919, 2007. 6972

Liu, H., Jacob, D. J., Bey, I., Yantosca, R., Duncan, B. N., and Sachse, G. W.: Transport pathways for Asian pollution outflow over the Pacific: interannual and seasonal variations, J. Geophys. Res., 108, 8786, doi:10.1029/2002JD003102, 2003. 6972

Liu, J. J., Jones, D. B. A., Worden, J. R., Noone, D., Parrington, M., and Kar, J.: Analysis of the summertime buildup of tropospheric ozone abundances over the Middle East and North Africa as observed by the Tropospheric Emission Spectrometer instrument, J. Geophys. Res., 114, D05304, doi:10.1029/2008JD010993, 2009. 6970

Ojha, N., Pozzer, A., Rauthe-Schöch, A., Baker, A. K., Yoon, J., Brenninkmeijer, C. A. M., and Lelieveld, J.: WRF-Chem simulations of ozone and CO over India during the summer monsoon: Regional emissions and transport, Atmos. Chem. Phys. Discuss., submitted, 2015. 6993

O'Sullivan, D. A.: Temporal and spatial variability of halogenated compounds and other trace gases, Ph.D. thesis, University of East Anglia, Norwich, United Kingdom, 2007. 6973

Pan, L., Crawford, J., Tanimoto, H., Lawrence, M., Panday, A., Babu, S. S., Barret, B., Schlager, H., Konopka, P., and Bian, J.: Report on the Atmospheric Composition and the summer Asian Monsoon (ACAM) workshop, 9–12 June 2013, Kathmandu, Nepal, SPARC Newsletter, 42, 40–45, 2014. 6971

Park, M., Randel, W. J., Emmons, L. K., Bernath, P. F., Walker, K. A., and Boone, C. D.: Chemical isolation in the Asian monsoon anticyclone observed in Atmospheric Chemistry Experi-

ment (ACE-FTS) data, Atmos. Chem. Phys., 8, 757–764, doi:10.5194/acp-8-757-2008, 2008. 6970, 6989, 6991

Parrish, D. D., Holloway, J. S., Trainer, M., Murphy, P. C., Fehsenfeld, F. C., and Forbes, G. L.: Export of North American ozone pollution to the North Atlantic ocean, Science, 259, 1436–1439, doi:10.1126/science.259.5100.1436, 1993. 6980

Parrish, D. D., Trainer, M., Holloway, J. S., Yee, J. E., Warshawsky, M. S., Fehsenfeld, F. C., Forbes, G. L., and Moody, J. L.: Relationships between ozone and carbon monoxide at surface sites in the North Atlantic region, J. Geophys. Res., 103, 13357–13376, doi:10.1029/98JD00376, 1998. 6980

Patra, P. K., Niwa, Y., Schuck, T. J., Brenninkmeijer, C. A. M., Machida, T., Matsueda, H., and Sawa, Y.: Carbon balance of South Asia constrained by passenger aircraft CO_2 measurements, Atmos. Chem. Phys., 11, 4163–4175, doi:10.5194/acp-11-4163-2011, 2011. 6972

Randel, W. J. and Jensen, E. J.: Physical processes in the tropical tropopause layer and their roles in a changing climate, Nature Geosci., 6, 169–176, doi:10.1038/ngeo1733, 2013. 6970, 6989

Randel, W. J. and Park, M.: Deep convective influence on the Asian summer monsoon anticyclone and associated tracer variability observed with Atmospheric Infrared Sounder (AIRS), J. Geophys. Res., 111, D12314, doi:10.1029/2005JD006490, 2006. 6970, 6990

Randel, W. J., Park, M., Emmons, L., Kinnison, D., Bernath, P., Walker, K. A., Boone, C., and Pumphrey, H.: Asian monsoon transport of pollution to the stratosphere, Science, 328, 611–613, doi:10.1126/science.1182274, 2010. 6971

Roiger, A.: private communication, 2014. 6994

Sahu, L. K., Lal, S., Thouret, V., and Smit, H. G.: Climatology of tropospheric ozone and water vapour over Chennai: a study based on MOZAIC measurements over India, Int. J. Climatol., 31, 920–936, doi:10.1002/joc.2128, 2011. 6983

Sahu, L. K., Sheel, V., Kajino, M., Deushi, M., Gunthe, S. S., Sinha, P. R., Sauvage, B., Thouret, V., and Smit, H. G.: Seasonal and interannual variability of tropospheric ozone over an urban site in India: a study based on MOZAIC and CCM vertical profiles over Hyderabad, J. Geophys. Res., 119, 3615–3641, doi:10.1002/2013JD021215, 2014. 6983

Scharffe, D., Slemr, F., Brenninkmeier, C. A. M., and Zahn, A.: Carbon monoxide measurements onboard the CARIBIC passenger aircraft using UV resonance fluorescence, Atmos. Meas. Tech., 5, 1753–1760, doi:10.5194/amt-5-1753-2012, 2012. 6974

Scheeren, H. A., Lelieveld, J., Roelofs, G. J., Williams, J., Fischer, H., de Reus, M., de Gouw, J. A., C.Warneke, Holzinger, R., Schlager, H., Klüpfel, T., Bolder, M., van der Veen, C., and Lawrence, M.: The impact of monsoon outflow from India and Southeast Asia in the upper troposphere over the eastern Mediterranean, Atmos. Chem. Phys., 3, 1589–1608, doi:10.5194/acp-3-1589-2003, 2003. 6970

Schuck, T. J., Brenninkmeijer, C. A. M., Slemr, F., Xueref-Remy, I., and Zahn, A.: Greenhouse gas analysis of air samples collected onboard the CARIBIC passenger aircraft, Atmos. Meas. Tech., 2, 449–464, doi:10.5194/amt-2-449-2009, 2009. 6973, 6975

Schuck, T. J., Brenninkmeijer, C. A. M., Baker, A. K., Slemr, F., van Velthoven, P. F. J., and Zahn, A.: Greenhouse gas relationships in the Indian summer monsoon plume measured by the CARIBIC passenger aircraft, Atmos. Chem. Phys., 10, 3965–3984, doi:10.5194/acp-10-3965-2010, 2010. 6971, 6973, 6984, 6986, 6989, 6991

Sheel, V., Sahu, L. K., Kajino, M., Deushi, M., Stein, O., and Nedelec, P.: Seasonal and interannual variability of carbon monoxide based on MOZAIC observations, MACC reanalysis, and model simulations over an urban site in India, J. Geophys. Res., 119, 9123–9141, doi:10.1002/2013JD021425, 2014. 6984, 6992

Spivakovsky, C. M., Logan, J. A., Montzka, S. A., Balkanski, Y. J., Foreman-Fowler, M., Jones, D. B. A., Horowitz, L. W., Fusco, A. C., Brenninkmeijer, C. A. M., Prather, M. J., Wofsy, S. C., and McElroy, M. B.: Three-dimensional climatological distribution of tropospheric OH: update and evaluation, J. Geophys. Res., 105, 8931–8980, doi:10.1029/1999JD901006, 2000. 6988

Stohl, A., Forster, C., Frank, A., Seibert, P., and Wotawa, G.: Technical note: The Lagrangian particle dispersion model FLEXPART version 6.2, Atmos. Chem. Phys., 5, 2461–2474, doi:10.5194/acp-5-2461-2005, 2005. 6972, 6975

Stohl, A., Sodemann, H., Eckhardt, S., Frank, A., Seibert, P., and Wotawa, G.: The Lagrangian particle dispersion model FLEXPART version 8.2, Tech. rep., Norwegian Institute of Air Research (NILU), Kjeller, Norway, available at: http://flexpart.eu/, last access: 6 February 2015, 2010. 6975

Trainer, M., Parrish, D. D., Goldan, P. D., Roberts, J., and Fehsenfeld, F. C.: Review of observation-based analysis of the regional factors influencing ozone concentrations, Atmos. Environ., 34, 2045–2061, doi:10.1016/S1352-2310(99)00459-8, 2000. 6980

Traub, M. and Lelieveld, J.: Cross-tropopause transport over the eastern Mediterranean, J. Geophys. Res., 108, 4712, doi:10.1029/2003JD003754, 2003. 6970

Umezawa, T., Baker, A. K., Oram, D., Sauvage, C., O'Sullivan, D., Rauthe-Schöch, A., Montzka, S. A., Zahn, A., and Brenninkmeijer, C. A. M.: Methyl chloride in the upper troposphere observed by the CARIBIC passenger aircraft observatory: large-scale distributions and Asian summer monsoon outflow, J. Geophys. Res., 119, 5542–5558, doi:10.1002/2013JD021396, 2014. 6971

Voulgarakis, A., Telford, P. J., Aghedo, A. M., Braesicke, P., Faluvegi, G., Abraham, N. L., Bowman, K. W., Pyle, J. A., and Shindell, D. T.: Global multi-year O_3–CO correlation patterns from models and TES satellite observations, Atmos. Chem. Phys., 11, 5819–5838, doi:10.5194/acp-11-5819-2011, 2011. 6980

Weigelt, A., Hermann, M., van Velthoven, P. F. J., Brenninkmeijer, C. A. M., Schlaf, G., Zahn, A., and Wiedensohler, A.: Influence of clouds on aerosol particle number concentrations in the upper troposphere, J. Geophys. Res., 114, D01204, doi:10.1029/2008JD009805, 2009. 6978

Xiong, X., Houweling, S., Wei, J., Maddy, E., Sun, F., and Barnet, C.: Methane plume over south Asia during the monsoon season: Satellite observation and model simulation, Atmos. Chem. Phys., 9, 783–794, doi:10.5194/acp-9-783-2009, 2009. 6970

Zahn, A., Brenninkmeijer, C. A. M., Asman, W. A. H., Crutzen, P. J., Heinrich, G., Fischer, H., Cuijpers, J. W. M., and van Velthoven, P. F. J.: Budgets of O_3 and CO in the upper troposphere: CARIBIC passenger aircraft results 1997–2001, J. Geophys. Res., 107, 4337, doi:10.1029/2001JD001529, 2002. 6980, 6991

Zahn, A., Weppner, J., Widmann, H., Schlote-Holubek, K., Burger, B., Kühner, T., and Franke, H.: A fast and precise chemiluminescence ozone detector for eddy flux and airborne application, Atmos. Meas. Tech., 5, 363–375, doi:10.5194/amt-5-363-2012, 2012. 6974

Zahn, A., Christner, E., van Velthoven, P. F. J., Rauthe-Schöch, A., and Brenninkmeijer, C. A. M.: Processes controlling water vapor in the upper troposphere / lowermost stratosphere: An analysis of eight years of monthly measurements by the IAGOS-CARIBIC observatory, J. Geophys. Res., 119, 11505–11525, doi:10.1002/2014JD021687, 2014. 6974

Ziereis, H., Schlager, H., Schulte, P., van Velthoven, P. F. J., and Slemr, F.: Distributions of NO, NO_x, and NO_y in the upper troposphere and lower stratosphere between 28° and 61° N during POLINAT 2, J. Geophys. Res., 105, 3653–3664, doi:10.1029/1999JD900870, 2000. 6974

Table 1. CARIBIC2 flights to Chennai/India in 2008. Listed are the flight number, date of departure and flight direction. Column 4 gives the northern cut-off for the trajectory analysis which was selected for each month to exclude trajectories belonging to the eastward jet stream. The last column lists the latitude of the wind reversal along each flight track which is used as indicator of centre latitude of the monsoon UTAC at flight altitude (see Fig. 3).

Flight no.	Direction	Date of departure	Northern cut-off	Monsoon centre latitude
236	southward	18 June 2008	36.5° N	27.9° N
237	northward	18 June 2008	36.5° N	25.5° N
238	southward	19 June 2008	36.5° N	25.8° N
239	northward	19 June 2008	36.5° N	24.4° N
240	southward	15 July 2008	40.0° N	26.7° N
241	northward	15 July 2008	40.0° N	26.1° N
244	southward	13 August 2008	40.0° N	26.6° N
245	northward	13 August 2008	40.0° N	24.6° N
246	southward	14 August 2008	40.0° N	25.8° N
247	northward	14 August 2008	40.0° N	25.3° N
248	southward	10 September 2008	35.5° N	23.5° N
249	northward	10 September 2008	35.5° N	22.7° N
250	southward	11 September 2008	35.5° N	24.9° N
251	northward	11 September 2008	35.5° N	24.0° N

Table 2. Receptor regions used in the analysis of the FLEXPART forward trajectories.

Name	Region
North America	30–50° N, 150–70° W
Central Pacific	10–34° N, 130° E–150° W
Central Africa	0–25° N, 10° W–35° E
Mediterranean	28–40° N, 0° E–40° W
South Asian monsoon	centre: 80° E*, radius: 38° longitude, 16° latitude
TP Stratosphere	higher than thermal tropopause along trajectory
PV Stratosphere	higher than dynamical tropopause (PV > 2.5 PVU) along trajectory

* Latitude of monsoon centre is flight dependent (see last column in Table 1).

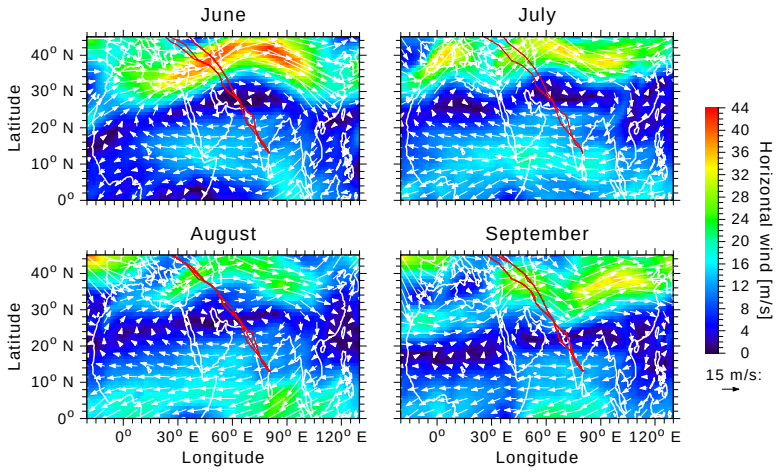

Figure 1. CARIBIC flight tracks across the South Asian monsoon region in June–September 2008. The panels show the flight tracks for each month and 10-day mean ECMWF horizontal wind fields at 250 hPa ending at the day of the last flight in each month. The colour code shows the wind speed while the white arrows indicate the wind direction. Note the anti-cyclonic monsoon circulation centred over the Indian subcontinent.

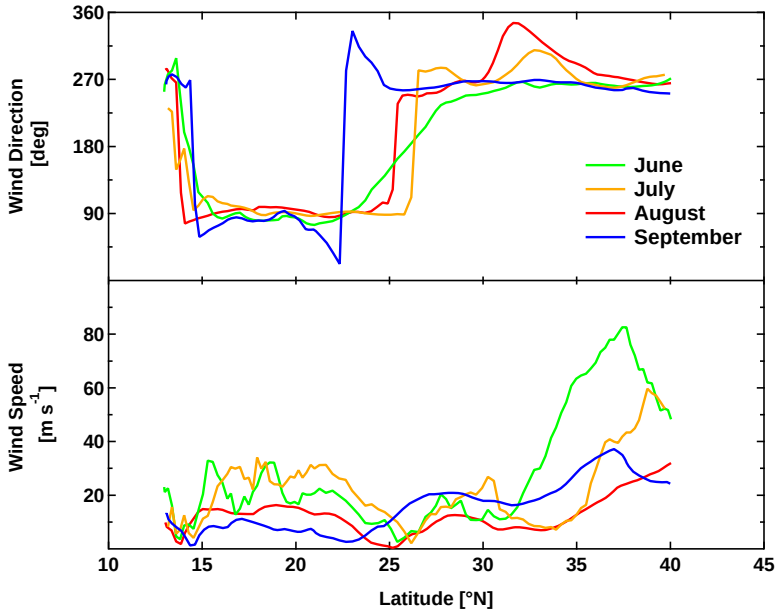

Figure 2. Latitudinal profiles of wind direction (top panel, 90° means wind from the east, 180° from the south, 270° from the west) and wind speed (bottom panel) at aircraft cruise altitude for the first flight from Frankfurt to Chennai in each of the four monsoon months.

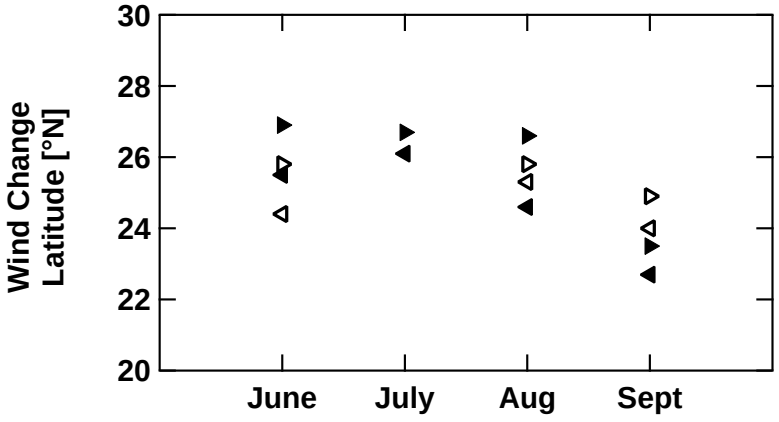

Figure 3. Latitude of the aircraft at the transition between eastward and westward flow in the UTAC for each flight during the summer monsoon 2008. Arrows pointing to the right indicate flights from Frankfurt to Chennai, arrows pointing to the left indicate return flights. Filled symbols represent the first round-trip flight series, open symbols indicate the second (when applicable).

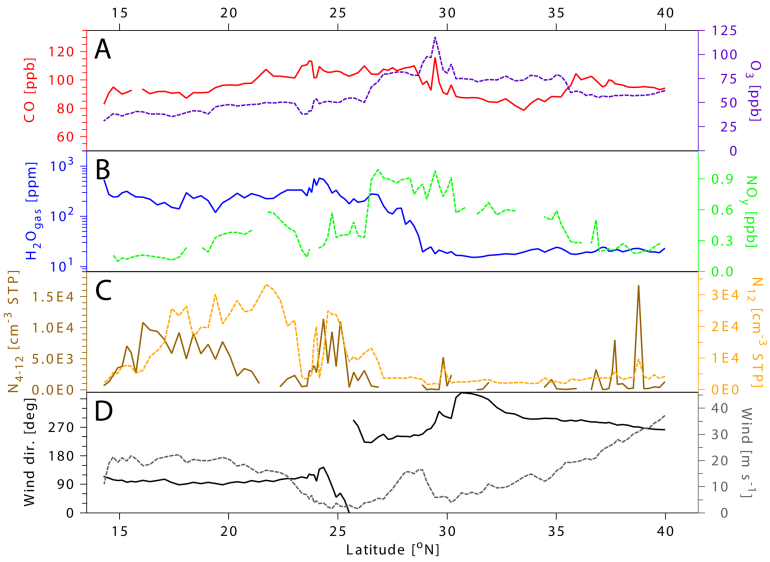

Figure 4. Latitudinal profiles of trace gases and meteorological parameters during the second flight in August from Frankfurt to Chennai on 14 August 2008. In addition to colour-coding of axes, scales for parameters represented by solid lines are on the left and scales for parameters represented by dashed lines are on the right. Aerosol particle number concentrations are given at STP (273.15 K, 1013.25 hPa). Note that all data is shown versus geographical latitude and that the water vapour shown in blue in panel B is on a logarithmic scale (see also Figs. S9–S21).

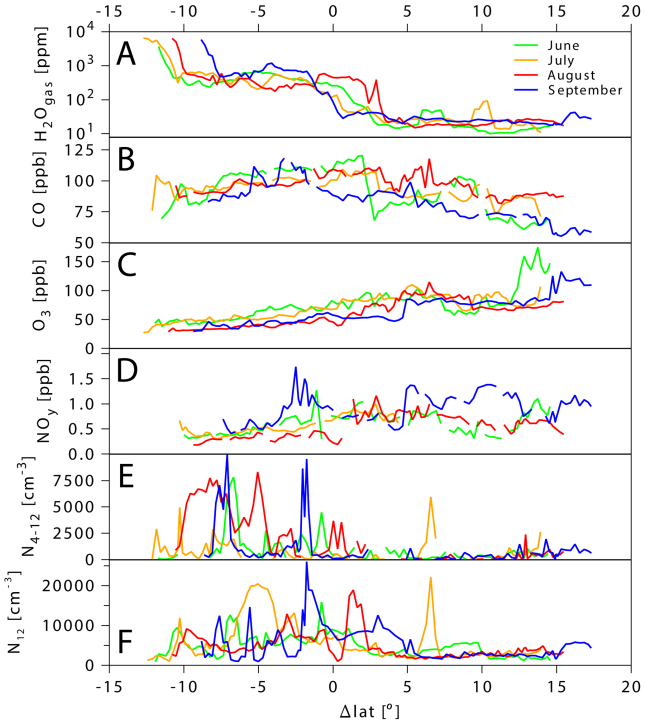

Figure 5. Profiles of trace gases **(a–d)** and aerosol particle number concentrations (**e** and **f**, at STP 273.15 K, 1013.25 hPa) vs. relative latitude (Δlat) coordinates for the first return flight from Chennai during each month. Note the logarithmic scale in the water vapour plot in **(a)** (see also Figs. S22–S24).

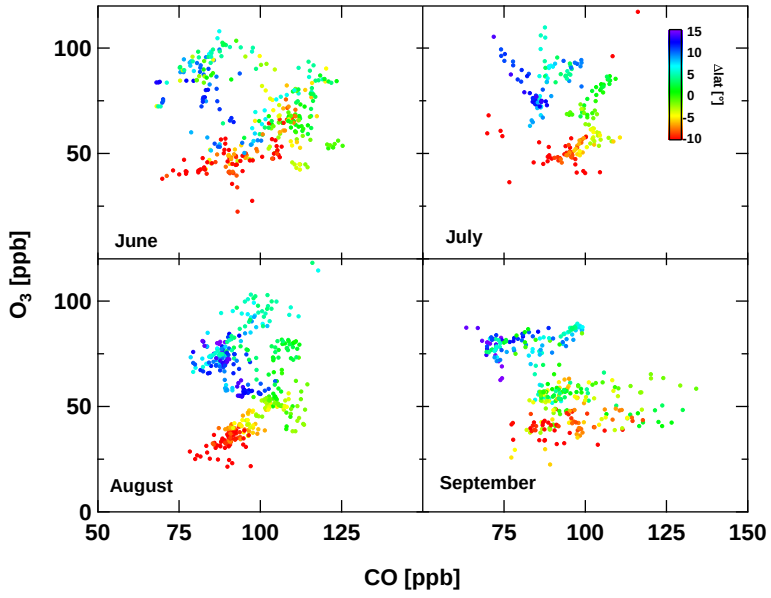

Figure 6. Monthly distributions of O_3 vs. CO during the summer monsoon season 2008. Points are colour-coded by relative position within the UTAC, as determined by Δlat (see also Sect. S6).

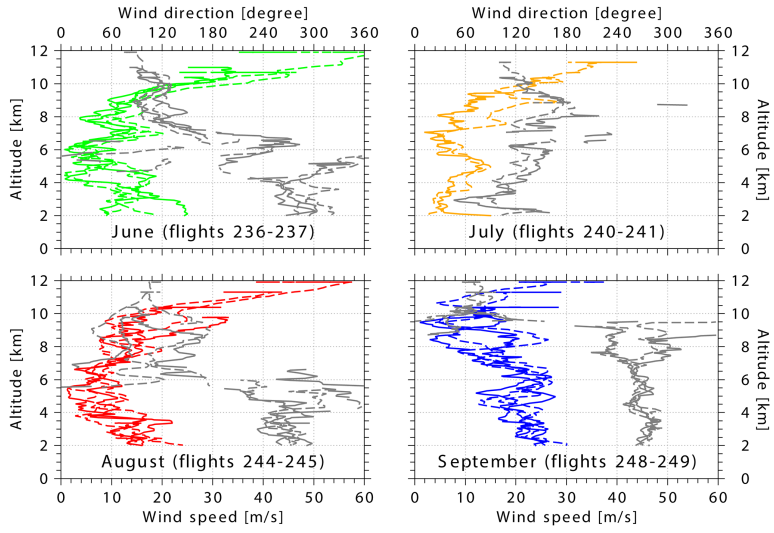

Figure 7. Wind speed (coloured lines, lower *x* axis) and wind direction (grey lines, upper *x* axis, 90° means wind from the east, 180° from the south, 270° from the west) from the measurements onboard the CARIBIC aircraft for the descent into (solid lines) and ascent from (dashed lines) Chennai. Only data south of 16° N and above 2 km altitude is plotted. Chennai is at 12.99° N, 80.18° E.

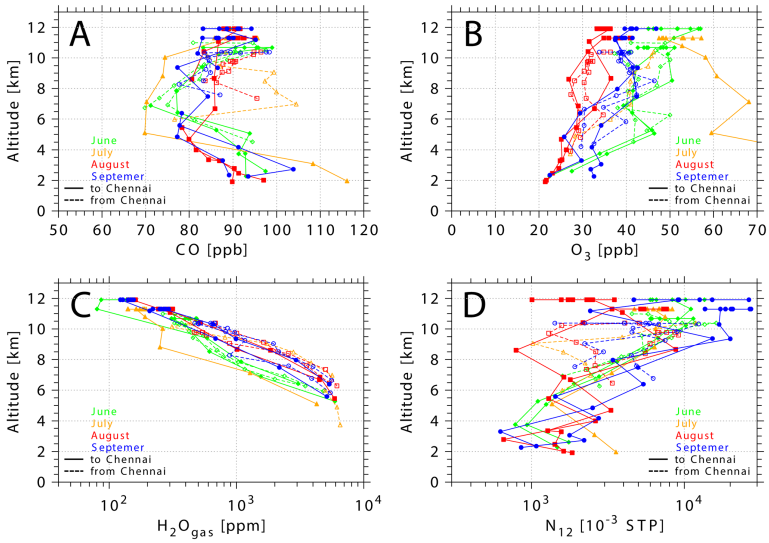

Figure 8. Vertical profiles of CO **(a)**, O_3 **(b)**, water vapour **(c)** and number concentration of Aitken mode aerosol particles N_{12} at STP (273.15 K, 1013.25 hPa; **d**) between 2 km and 12 km during descent into (solid lines and filled symbols) and ascent from (dashed lines and open symbols) Chennai.

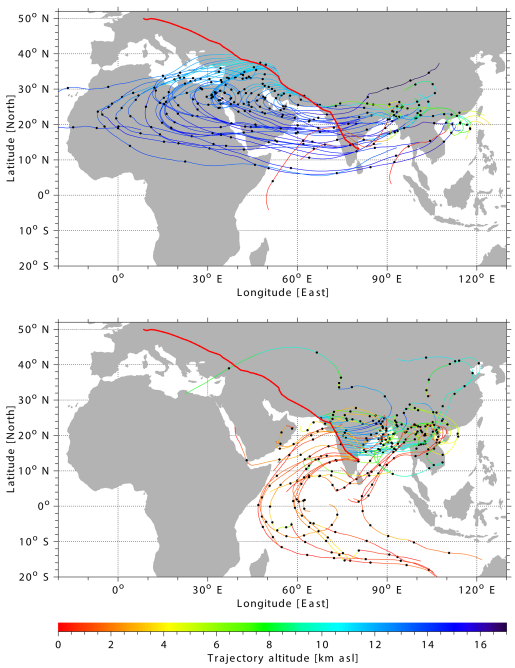

Figure 9. 10 day backward trajectories for CARIBIC flight 244 to Chennai on 13 August 2008. Upper panel: trajectories north of the wind reversal at 26.6° N. Lower panel: trajectories south of the wind reversal. Every second trajectory is plotted for clarity. The colour indicates the trajectory altitude and the black dots mark 24 h time steps along the trajectories. The CARIBIC flight track is shown by the thick red line (see also Figs. S29–S31).

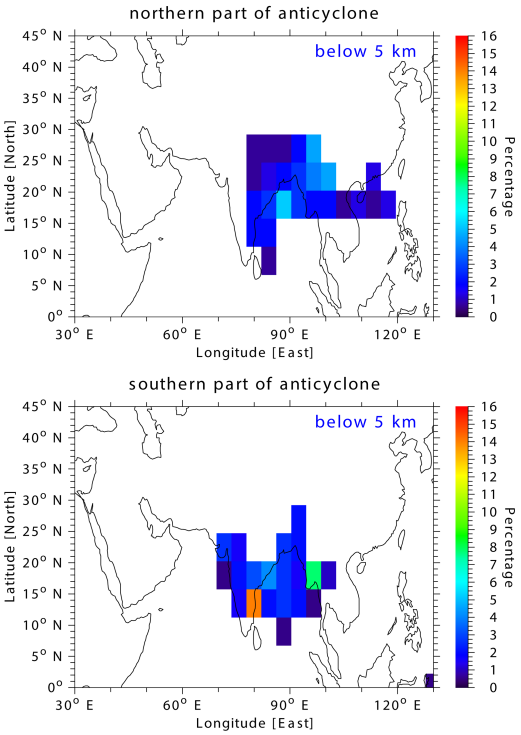

Figure 10. Distribution of source regions for the CARIBIC flights in August 2008. The colour code shows the percentage of trajectories that came from below 5 km altitude in the 4° × 4° grid boxes. Upper panel: source regions for trajectories starting north of the wind reversal. Lower panel: source regions for trajectories starting south of the wind reversal.

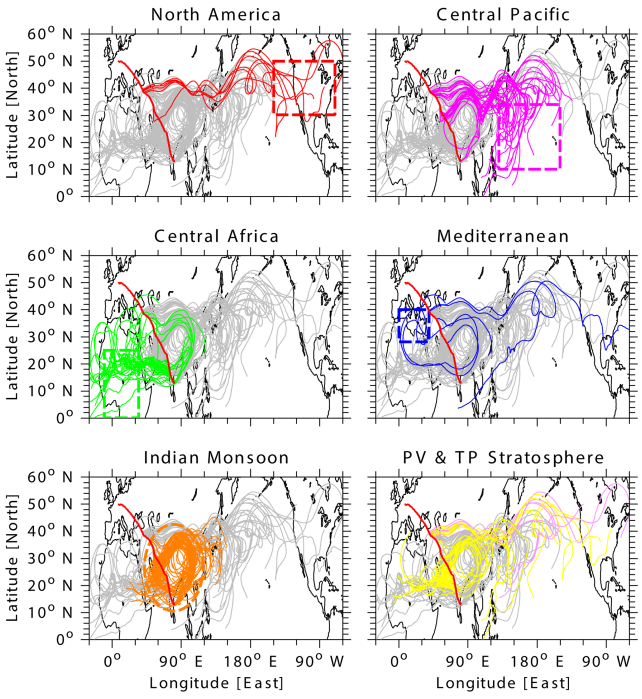

Figure 11. Receptor regions as determined for CARIBIC flight 244 to Chennai on 13 August 2008 (flight track shown with thick red solid line). The panels show all FLEXPART forward trajectories for this flight south of the northern cut-off (40° N) in grey. For each receptor region, the corresponding trajectories are shown in colour. The dashed lines indicate the boundaries of the receptor regions (boxes and ellipse). Trajectories with stratospheric parts are shown in the lower right panel in yellow for the thermal and pink for the dynamical tropopause criterion.

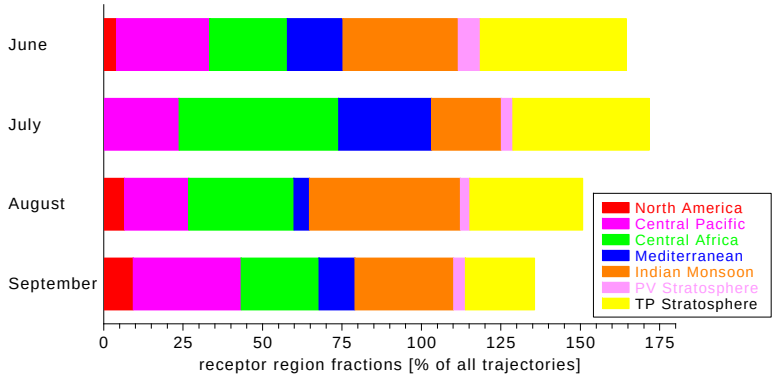

Figure 12. Receptor region fractions averaged over all CARIBIC flights to Chennai in June to September 2008. Since trajectories may reach multiple receptor regions, the totals exceed 100 %.

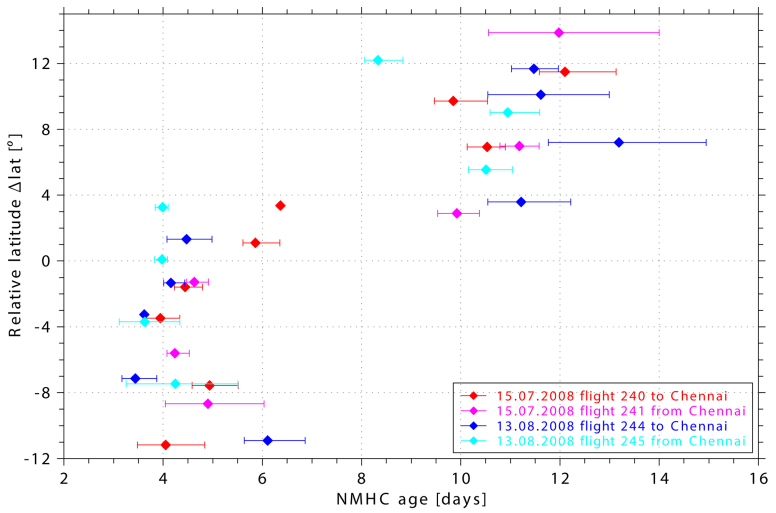

Figure 13. Photochemical age of pollutants in the air samples estimated from NMHC ratios (see Sect. 3.3.2 and Baker et al., 2011) versus relative latitude for the flights in July and the first two flights in August. Note the clustering of the chemically young samples close to and south of the wind reversal (Δlat $<\sim 3^{\circ}$) and the older more chemically processed samples further north. Shown are the mean chemical age together with the minimum and maximum age determined from the propane/ethane, n-butane/ethane and n-butane/propane ratios.

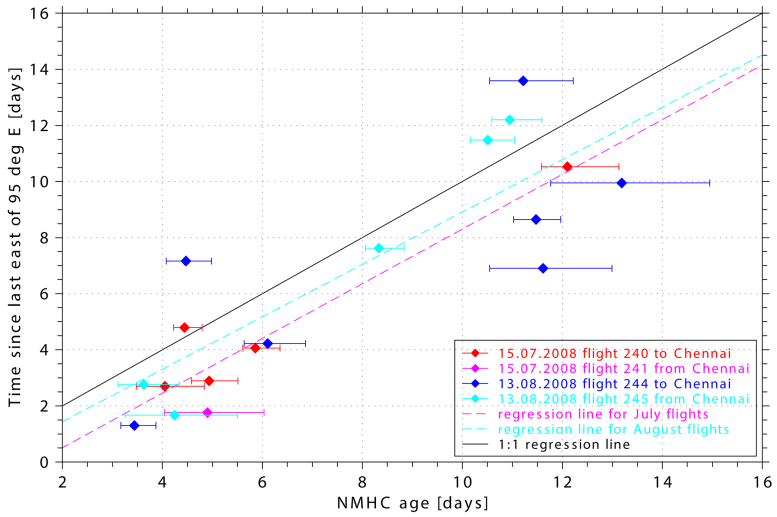

Figure 14. Comparison of the photochemical age of air estimated from NMHC ratios and the time the air had last been east of 95° E according to the FLEXPART trajectory calculations. Shown are the mean chemical age together with the minimum and maximum age determined from the propane/ethane, n-butane/ethane and n-butane/propane ratios. The colours indicate different flights (see legend). The black line indicates perfect agreement of both age estimates while the dashed lines indicate linear least-square regression lines of transport time and chemical ages derived from the different NMHC ratios (magenta regression lines for July, light blue for August flights).

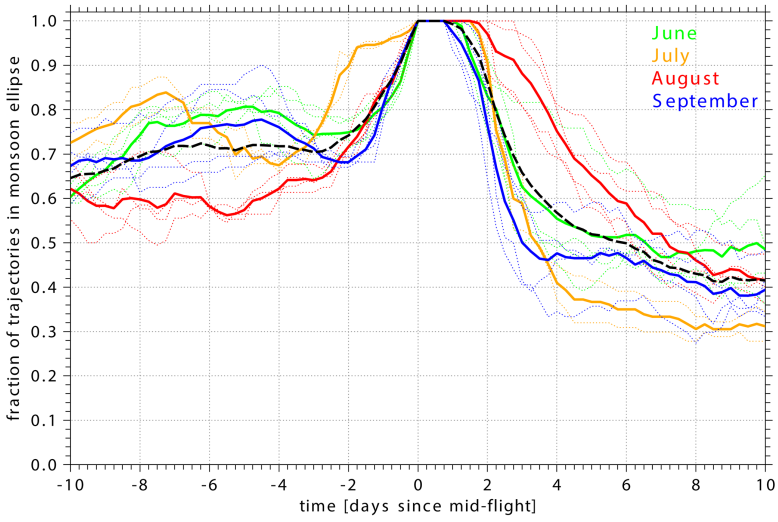

Figure 15. Monsoon leak rates for all flights between June and September 2008. Shown is the fraction of the backward and forward trajectories which started inside the monsoon ellipse (t = 0) and are inside the monsoon ellipse at the given time in days before and after the aircraft was inside the monsoon ellipse (see Sect. 3.3.3). The solid coloured lines are monthly means with the results from the single flights indicated by dotted lines. Colours indicate the months. The dashed black line shows the mean leak rate averaged over all flights.